A NEW HYSTERESIS MODEL BASED ON AN INTEGRAL TYPE DEFORMATION-HISTORY FOR ELASTOMERIC SEISMIC ISOLATION BEARINGS

H. KATO, T. MORI, N. MUROTA & S. SUZUKI
Bridgestone Corporation, Japan

M. KIKUCHI
Hokkaido University, Japan

SUMMARY:
A new hysteresis model for time history analysis of elastomeric seismic isolation bearings, using constitutive law with the same concept of finite element analysis (FEA) is proposed in the paper. The model has been developed based on an integral type deformation-history constitutive law for FEA which was previously proposed by the authors. First identification of the analytical model was conducted by the results of bi-directional loading test of scaled high-damping rubber bearings (HRB). Then, both shaking table test and numerical simulation by time history analysis of seismically isolated structure with the same HRB model was carried out. The test results showed good agreement with time history analysis using developed hysteresis model of the bearing. The applicability of the developed new hysteresis model for isolators was verified.

Keywords: Elastomeric Seismic Isolation Bearing, Hysteresis Model, Finite Element Analysis

1. INTRODUCTION

It is important to examine stress and strain distribution inside of elastomeric seismic isolation bearings under various dimensional loadings so as to study characteristics of isolation bearings. However, it is difficult to measure directly the stress and strain under large strains state by experimental methods. Therefore many studies on prediction of stress and strain in the body of elastomeric seismic isolation bearings by finite elemental analysis (FEA) have been conducted. In the study on FEA of rubber-like material, selection of a constitutive law is particularly important to reproduce nonlinear geometric and material effects. Especially, high-damping rubber bearings (HRB) have stronger nonlinear material effects than other bearings such as natural rubber bearings (NRB). Therefore, its restoring force characteristics are complicated. To reproduce restoring force characteristics of HRB, several constitutive laws have been presented. In our previous studies, we have proposed a new constitutive law of rubber-like material focusing on two important features of HRB as follows: properties of HRB depend little on its loading velocity and exhibit an elasto-plastic behaviour. On the other hands, it exhibits visco-elastic behaviours like creep. The constitutive law developed in our study is based on an integral type deformation-history (IDH) constitutive law, i.e., stress is relaxed depending on its equivalent strain. The constitutive law accurately reproduces complicated properties and creep-like behaviours of HRB.
FEA is a useful method to evaluate stress and strain inside distribution of elastomeric seismic isolation bearing. However, when we consider about numerical models for seismic response analysis, FEA is not adequate in practical use considering computation time and required power for pre/post process. Generally, seismic response analysis of seismically isolated buildings are conducted by time history analysis, and the restoring force characteristics of isolation bearings are simplified as an analytical model which consists of shear springs with non-linear hysteretic characteristics, without any consideration for geometric configuration. In previous studies, many analytical models of HRB, such as either normal or modified bi-linear model which takes shear strain dependency into account, Ramberg-Osgood model or Kikuchi-Aiken model, have been proposed. These models express properties of HRB under uni-dimensional horizontal loading. As examples of analytical models which

express properties of HRB under bi-directional shear loading, Yamamoto model, Wen model, Abe model or Grant model are given. Generally, Mechanical concepts of these models differ from those of FEA.

The purpose of this paper is to propose an analytical model for time history analysis, using constitutive law with the same concept of FEA. The model has been developed based on IDH constitutive law as mentioned above. The behaviour of bearings computed by the time history analysis with the model can be traced by FEA using same material constants and parameters, and detailed information, such as stress and strain distribution inside of bearing, will be obtained and will be fed back to design of isolation bearings.

2. PROPOSED HYSTERESIS MODEL

2.1. Integral Type Deformation-history (IDH) Constitutive Law

The IDH constitutive law is expressed as

$$\boldsymbol{S} = 2\Xi \frac{\partial W}{\partial \boldsymbol{C}} + 2\frac{\partial W_{\mathrm{vol}}}{\partial \boldsymbol{C}} + 2\sum_{\mathrm{n}=1}^{N} g_{\mathrm{n}} \int_{0}^{L} \frac{\mathrm{d}}{\mathrm{d}L'}\left(\frac{\partial \overline{W_0}}{\partial \boldsymbol{C}}\right) e^{-(L-L')/l_{\mathrm{n}}} \mathrm{d}L' \tag{2.1}$$

where $\boldsymbol{S}$ is the second Piola-Kirchhoff stress, $\boldsymbol{C}$ is the right Cauchy-Green tensor, W and $\overline{W_0}$ are strain energy density functions for deviatoric deformation related to elasticity and plasticity, respectively. W_{vol} is strain energy function for volumetric deformation, and g_{n} and l_{n} are material parameters. N is number of nonlinear elasto-plastic springs which will be described later. g_{n} is the ratio of loading stress to individual nonlinear elasto-plastic springs, and $\sum g_{\mathrm{n}}$ is equal to 1. L is the accumulated value of equivalent strain increment as follows:

$$L = \int_0^t \sqrt{\frac{2}{3}\boldsymbol{D}:\boldsymbol{D}}\,\mathrm{d}t \tag{2.2}$$

where $\boldsymbol{D}$ is the deviatoric part of the deformation rate tensor.

Ξ in Eqn 2.1 is the damage function to reproduce high modulus in small strain as follows:

$$\Xi = \theta + (1-\theta)\exp(-\frac{\lambda_{\max}}{\beta}) \tag{2.3}$$

where θ is the ratio of undamaged nonlinear elastic springs and β is the value of strain that the stress of damaged nonlinear elastic spring decrease from the initial value to the $1/e$ of the initial value. $\lambda_{\max}$ is the parameter calculated from maximum experienced principal stretch ratio as follows:

$$\lambda_{\max} = \max\left(\lambda_1 - \frac{1}{\lambda_1}\right) \tag{2.4}$$

where λ_1 is the maximum principal stretch ratio. In this paper, we use first and second member of the Yeoh model as strain energy density functions W and the Neo-Hookean model as strain energy density functions $\overline{W_0}$. W and $\overline{W_0}$ are shown in Eqn. 2.5. and 2.6, respectively.

$$W = a(I_1 - 3) + b(I_1 - 3)^2 \tag{2.5}$$
$$\overline{W_0} = c(\bar{I}_1 - 3) \tag{2.6}$$

where I_1 and $\bar{I}_1$ are the strain invariant and the deviatoric strain invariant, respectively. a, b and c are the material parameters.

Fig. 2.1 illustrates the concept of this constitutive law. The first member of right side of the equation corresponds to the part of nonlinear elastic spring, and the third member corresponds to the part of nonlinear elasto-plastic spring. One of the features of this constitutive law is that the force of nonlinear elasto-plastic springs relaxes corresponding to its deformation history. For example, when incremental stress ΔS_t is generated through small incremental time Δt, the ΔS_t is decreasing with its deformation history L. When incremental quantity of deformation history L reaches l_n, the ΔS_t relaxes to $\Delta S_t/e$. In this constitutive law, present stress is calculated by the convolution of incremental stress like ΔS_t.

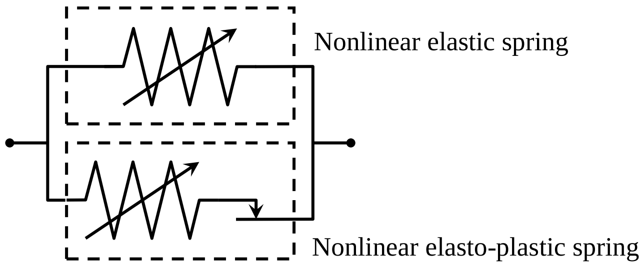

Figure 2.1. Concept of IDH constitutive law

2.2 Bi-directional Analytical Model for Time History Analysis

The constitutive law indicated in Eqn. 2.1. is defined in six degrees of freedom. Therefore, in the case of using this constitutive law as an analytical model for time history analysis, it is needed to reduce the degrees of freedom to bi-directional shear deformation components. Shear stress τ_1 and τ_2 related to shear strain γ_1 and γ_2 are given by

$$\tau_1(\gamma_1,\gamma_2) = \Xi(\gamma_1,\gamma_2)\cdot\gamma_1\left\{a^* + b^*\left(\gamma_1^2+\gamma_2^2\right)\right\} + \sum_{n=1}^{2}\frac{c_n^*}{3}\left\{\zeta_{n,1}(\gamma_1,\gamma_2) - \gamma_1\eta_n(\gamma_1,\gamma_2)\right\} \tag{2.7}$$

$$\tau_2(\gamma_1,\gamma_2) = \Xi(\gamma_1,\gamma_2)\cdot\gamma_2\left\{a^* + b^*\left(\gamma_1^2+\gamma_2^2\right)\right\} + \sum_{n=1}^{2}\frac{c_n^*}{3}\left\{\zeta_{n,2}(\gamma_1,\gamma_2) - \gamma_2\eta_n(\gamma_1,\gamma_2)\right\} \tag{2.8}$$

where, to simplify the expressions, several variables are replaced as follows: $2a\rightarrow a^*$, $4b\rightarrow b^*$, $2gc\rightarrow c^*$, $\sqrt{3}L\rightarrow\Gamma$, $\sqrt{3}l\rightarrow l^*$. And, in this paper, the number of nonlinear elasto-plastic springs N is set as 2. $\zeta_{n,1}$, $\zeta_{n,2}$ and η_n are given as results of curvilinear integral along the deformation orbit χ as follows.

$$\zeta_{n,1}(\gamma_1,\gamma_2) = \int_\chi \frac{d}{d\Gamma'}\left[\gamma_1'\left(\gamma_1'^2+\gamma_2'^2+3\right)\right]e^{-\frac{\Gamma-\Gamma'}{l_n^*}}\,d\Gamma' \tag{2.9}$$

$$\zeta_{n,2}(\gamma_1,\gamma_2) = \int_\chi \frac{d}{d\Gamma'}\left[\gamma_2'\left(\gamma_1'^2+\gamma_2'^2+3\right)\right]e^{-\frac{\Gamma-\Gamma'}{l_n^*}}\,d\Gamma' \tag{2.10}$$

$$\eta_n(\gamma_1,\gamma_2) = \int_\chi \frac{d}{d\Gamma'}\left[\left(\gamma_1'^2+\gamma_2'^2\right)\right]e^{-\frac{\Gamma-\Gamma'}{l_n^*}}\,d\Gamma' \tag{2.11}$$

The accumulated value Γ of equivalent strain increment is expressed as

$$\Gamma = \int_\chi |ds| \tag{2.12}$$

Ξ is the damage function whose degrees of freedom are reduced as follows:

$$\Xi = \theta + (1-\theta)\exp\left(-\frac{\gamma_{max}}{\beta}\right) \tag{2.13}$$

where γ_{max} is the parameter calculated from maximum experienced shear strain expressed as follows:

$$\gamma_{max} = \max_{\chi}\left(\sqrt{\gamma_1^2 + \gamma_2^2}\right) \tag{2.14}$$

As mentioned above, the analytical model for time history analysis under bi-directional loadings based on an elasto-plastic, IDH constitutive law is derived.

3. BI-DIRECTIONAL LOADING TEST OF HIGH-DAMPING RUBBER BEARINGS

Bi-directional loading test of HRB was carried out for the identification of material parameters. In this chapter, the tests and the parameters identification are described in detail.

3.1. Test Specimen

Test specimen subjected to the loading test is shown in Fig. 3.1. The diameter of the specimen is 225mm, the thickness of inner rubber is 1.6mm, the number of layers is 28 and the thickness of shim plate is 1.0mm. First shape factor S_1 is 35.2 and second shape factor S_2, which is given by dividing effective diameter by total rubber height, is 5.02. These values of S_1 and S_2 are typical for isolation bearings used in Japan. The isolator used for this test had shear modulus of 0.62 N/mm^2 and equivalent damping ratio of 0.24 at shear strain γ=1.0, under loading frequency f=0.33Hz and temperature T=20 Celsius degree.

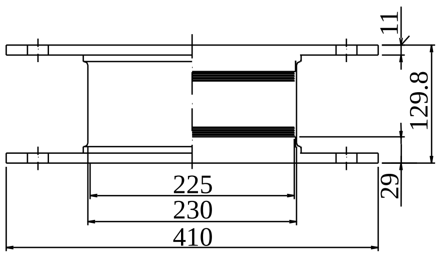

Figure 3.1. Test specimen for bi-directional loading test: All units are in mm.

3.2. Test Method

Test program is shown in Table. 3.1. Orbits for uni- and bi-directional displacement-controlled tests are also shown in Fig. 3.2. The transverse diameter of the elliptic orbit in Fig. 3.2. (b) is twice of the conjugate diameter, and the circled number in the figure corresponds to the sequence of the motion. Maximum shear strain of the major axis was increased gradually from 0.1 to 4.0. Test frequency was 0.33Hz in sinusoidal wave. Number of cycle was 3 in major axis. Vertical compression stress was kept constant as 15N/mm^2 during shear-loading. Specimen was used one by one in each test.

Table 3.1. Test program

Direction	Maximum shear strain (γ_x, γ_y)	Frequency (f_x, f_y) (Hz)
Uni-direction (Linear orbit)	(±0.1,0)×3→(±0.2,0)×3→(±0.5,0)×3 →(±1.0,0)×3→(±1.5,0)×3→(±2.0,0)×3 →(±2.5,0)×3→(±3.0,0)×3→(±4.0,0)×3	(0.33, -)
Bi-direction (Elliptic orbit)	(±0.1, ±0.05)×3→(±0.2, ±0.1)×3→(±0.5, ±0.25)×3 →(±1.0, ±0.5)×3→(±1.5, ±0.75)×3→(±2.0, ±1.0)×3 →(±2.5, ±1.25)×3→(±3.0, ±1.5)×3→(±4.0, ±2.0)×3	(0.33, 0.33)

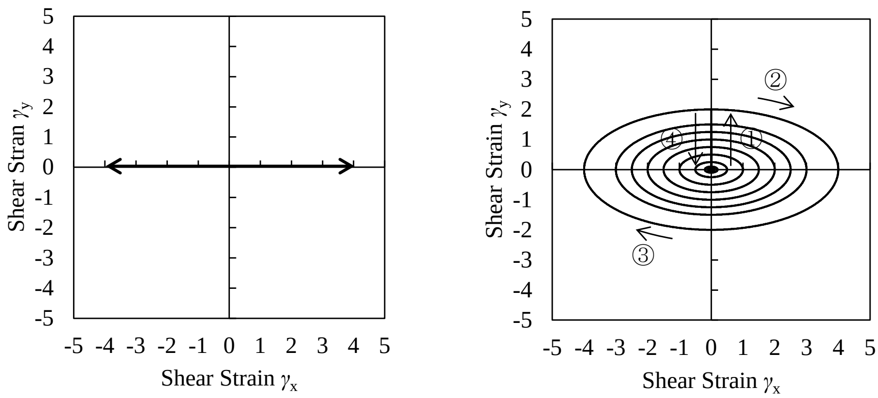

(a) Uni-direction (Linear) (b) Bi-direction (Elliptic)

Figure 3.2. Orbits for uni- and bi-directional displacement-controlled tests: The circled number in the figure corresponds to the sequence of the motion.

3.3. Test Results

Material parameters, a^*, b^*, c_1^*, c_2^*, l_1^*, l_2^*, θ and β were calibrated by nonlinear least-squares method, based on the characteristics of isolators, shear modulus and equivalent damping ratio, computed from the test results. Table 3.2 summarizes the identified material parameters. A comparison of stress-strain relationships between the test results and the analytical results using these material parameters are shown in Fig. 3.3. To compare these results, stress-strain relationships calculated by finite element model which had the same configuration as the specimen is shown in Fig. 3.4. A constitutive law of finite element model was the elasto-plastic, IDH constitutive law introduced in section 2.1. Material parameters used in the finite element model were identical to those of analytical model. The analytical results shows good agreement with the test results, likewise, with the results by FEA. This result indicates that mechanical characteristics of isolator are mostly governed by shear deformation. Therefore the analytical model defined in two degrees of freedom has enough accuracy to represent the characteristics of isolators.

Table 3.2. Material parameters for analytical model of HRB

a^* (N/mm^2)	b^* (N/mm^2)	c_1^* (N/mm^2)	c_2^* (N/mm^2)	l_1	l_2	θ	β
0.7189	0.02796	3.237	0.5128	0.03006	0.3592	0.3696	0.4578

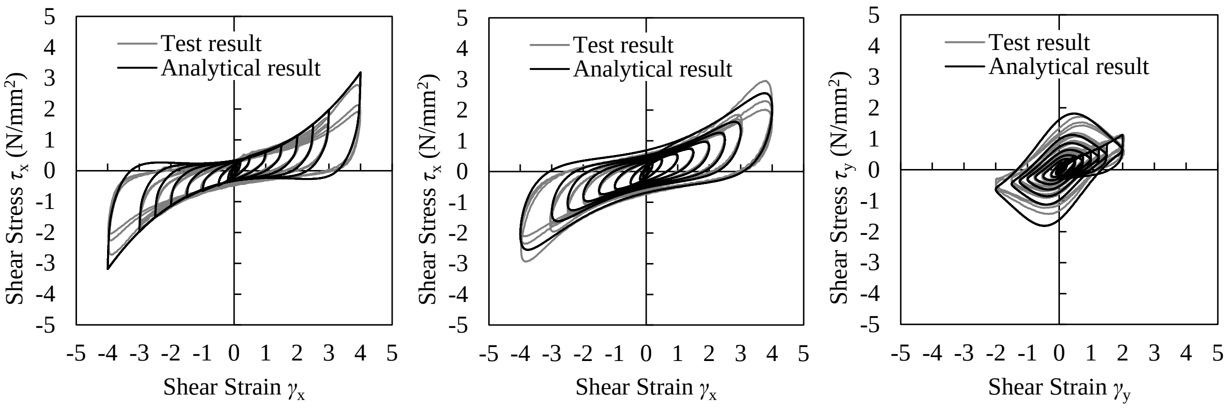

(a) Uni-direction (b) Bi-direction (major axis) (c) Bi-direction (minor axis)

Figure 3.3. Stress-strain relationships obtained by test and analytical model

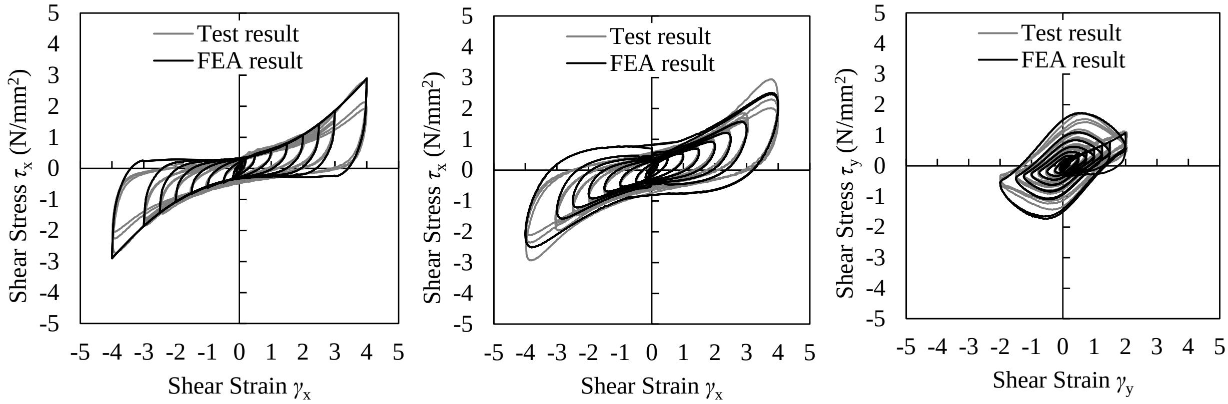

(a) Uni-direction (b) Bi-direction (major axis) (c) Bi-direction (minor axis)

Figure 3.4. Stress-strain relationships obtained by test and finite element model

4. SHAKING TABLE TEST

In order to verify the analytical model described in chapter 2 and 3, we conducted shaking tests of seismically isolated structure with HRB, and compared test results and analytical results using the proposed model.

4.1. Test Specimen

Schematic view of test and analytical model is shown in Fig. 4.1. Test model had a four-floor steel frame on bay in each horizontal direction, and the seismic isolation system composed of four HRBs was arranged below the first story. The dimensional scale factor was set as 1/4. The cross-sectional dimensions of girders, columns and beams were H150mm × 150mm × 7mm ×10mm. The seismic reactive masses assigned in the first, second and third story, and top floor of the superstructure were equal to 5kN-sec^2/m, 4kN-sec^2/m, 4kN-sec^2/m and 4kN-sec^2/m respectively, which were appropriately simulated by rigid slabs and supplemental mass blocks. The vertical load exerting on each isolator was equal to 41.7kN.

The outer diameter of the isolator using the test was 150mm, the inner diameter was 10mm, the thickness of inner rubber was 2mm, the number of inner rubber was 25 and the thickness of shim plate was 1.2mm. The first and second shape factor of the isolator was 17.5 and 3.0, respectively. These values are smaller than typical values in Japan, in order to adjust a natural period of seismic isolation system by decreasing the shear stiffness of the isolator. The isolator had the same material properties as those of the isolator discussed in chapter 3. The natural period of this seismically structure was adjusted as 0.9sec at shear strain γ=1. The compressive stress on each isolator was designed as 2.4N/mm^2.

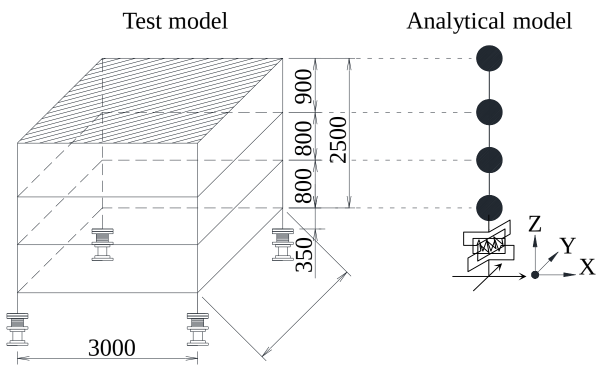

Figure 4.1. Model structure for shaking table test and analysis

4.2. Test Program

Test program is presented in Table 4.1. The typical earthquake records were chosen, of which the predominant period was shorter than 1.0second: JMA-KOBE and KOKUJI, longer than 2.5seconds: SANNOMARU. Here, KOKUJI is an artificial ground motion based on the spectra officially announced by the Ministry of Land, Infrastructure and Transport. The signal used in this study was arranged so as to have the same phase of 1968 HACHINOHE (EW) record without considering any amplification by soil. SANNOMARU is an artificial ground motion of which the long-period component was dominant. The signal was developed by Chubu Regional Bureau of Aichi Prefecture, and Nagoya City, assuming the Tokai-earthquake expected in the Tokai district. These seismic inputs were magnified so that the shear strain of the isolators would achieve 0.5 to 2.0. The scale factor of 1/2 for time step of input excitation was applied where the scale factor for dimension was 1/4. Five per cent-damped response spectra for each seismic excitation are shown in Fig. 4.2.

Table 4.1. Test program

Input signal	Shaking direction	P.G.A (m/sec^2)	Test scale (%)
JMA-KOBE	uni-direction (NS component)	8.18	52~230
	bi-direction	NS: 8.18, EW: 6.17	52~180
KOKUJI	uni-direction (EW component)	3.66	100~300
SANNOMARU	uni-direction (EW component)	1.86	100~250
	bi-direction	NS: 1.66, EW: 1.86	100~200

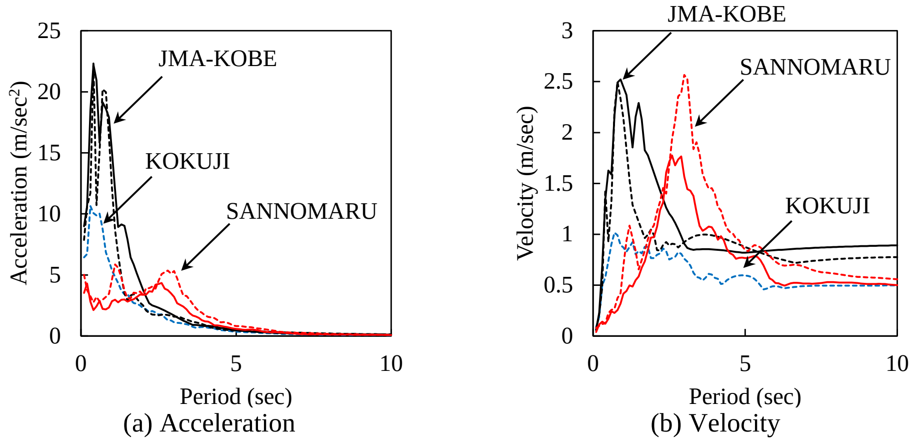

Figure 4.2. Five per cent-damped response spectra (Full size): solid line, NS component; dashed line, EW component.

4.3. Analytical Model

Analytical model consists of equivalent shear spring model with 4 lumped masses. In order to define the shear stiffness of each story, FEA of the superstructure was conducted using beam elements, and the results are summarized in Table 4.2. The structural damping of superstructure was set as 2%. Fourth-order Runge-Kutta formula was adopted for the time integration of the analysis, where time step was set as 0.5msec.

The restoring force characteristics of the isolator were expressed with the analytical model for time history analysis proposed in chapter 2. The material parameters of the HRB shown in Table 3.2. are values when temperature of the isolator is 20 Celsius degrees. Generally, shear modulus and equivalent damping ratio of HRB tend to be decreasing with temperature increasing. As the testing was conducted at room temperature, the effect of temperature on the characteristics of HRB shall be considered. Material parameters, which were used for the analysis, in consideration of temperature dependence are shown in Table 4.3.

Table 4.2. Shear stiffness of each story

Story	Shear stiffness (kN/mm)	
	X-direction	Y-direction
4	22.5	26.2
3	39.2	39.3
2	49.9	45.2
1	Isolated layer	

Table 4.3. Material parameters in consideration of temperature dependence

a^* (N/mm^2)	b^* (N/mm^2)	c_1^* (N/mm^2)	c_2^* (N/mm^2)	l_1	l_2	θ	β
0.7142	0.02778	2.950	0.4674	0.03006	0.3592	0.3696	0.4578

4.4. Comparison of Test Result and Analytical Result

The maximum response acceleration and displacement in the test and analysis are shown in Table 4.4. The analytical results show good agreement with the testing results. As an example, comparison of maximum response acceleration of each story under SANNOMARU (200%) in the experiment and analysis are shown in Fig 4.3., and stress-strain relationships of the HRB are shown in Fig 4.4. In Fig 4.4., the stresses in the test are averaged results of individual HRB. Testing program was consecutively conducted using same isolators; therefore, the isolators had experienced stiffness degradation due to fatigue effect. In addition, compressive stress of each isolator, 2.4N/mm^2, was smaller than that of the loading test conducted for identification of the material parameters proposed in Table 4.3. Generally, elastomeric isolators have significant dependence on compressive stress. In consideration of these effects, the analytical results show good agreement with test results.

Under JMA KOBE, maximum response displacement under uni-directional excitation tends to be larger than under bi-directional excitation. On the other hand, under SANNOMARU, maximum response displacement under uni-directional excitation tends to be smaller than under bi-directional excitation. In SANNOMARU (200%), the increasing ratio was the largest. The maximum response displacement under bi-directional excitation was about 1.08 times larger than that of under uni-directional excitation. It is likely to be due to characteristics of excitation. Generally, time history analysis of base isolation design is conducted in uni-directional excitation. Therefore, this result suggests that appropriate safety factor shall be counted in the analysis result.

Table 4.4. Seismic response under uni-/ bi-directional excitation

Input signal	Shaking Direction	Scale (%)	Test		Analysis	
			Maximum response acc. (m/sec^2)	Maximum response disp. (m)	Maximum response acc. (m/sec^2)	Maximum response disp. (m)
JMA-KOBE	Uni-direction (NS)	52	2.18	0.028	2.73	0.030
		104	3.38	0.052	4.33	0.061
		180	4.11	0.077	5.57	0.087
		210	4.69	0.090	6.70	0.101
		230	5.11	0.100	7.55	0.111
	Bi-direction (NS, EW)	52	2.21, 1.68	0.025, 0.019	2.40, 2.04	0.028, 0.021
		104	2.76, 2.33	0.047, 0.037	3.42, 3.49	0.054, 0.044
		180	3.30, 2.97	0.075, 0.050	4.86, 4.25	0.085, 0.059
KOKUJI	Uni-direction (EW)	100	2.25	0.024	2.24	0.027
		200	2.94	0.048	4.18	0.058
		300	4.16	0.070	4.77	0.079
SANNO -MARU	Uni-direction (EW)	100	2.09	0.029	2.42	0.031
		200	3.42	0.068	3.38	0.063
		250	4.35	0.098	4.40	0.093
	Bi-direction (NS, EW)	100	2.13, 1.98	0.034, 0.030	2.08, 2.21	0.038, 0.035
		200	4.64, 3.59	0.103, 0.078	5.22, 3.39	0.108, 0.074

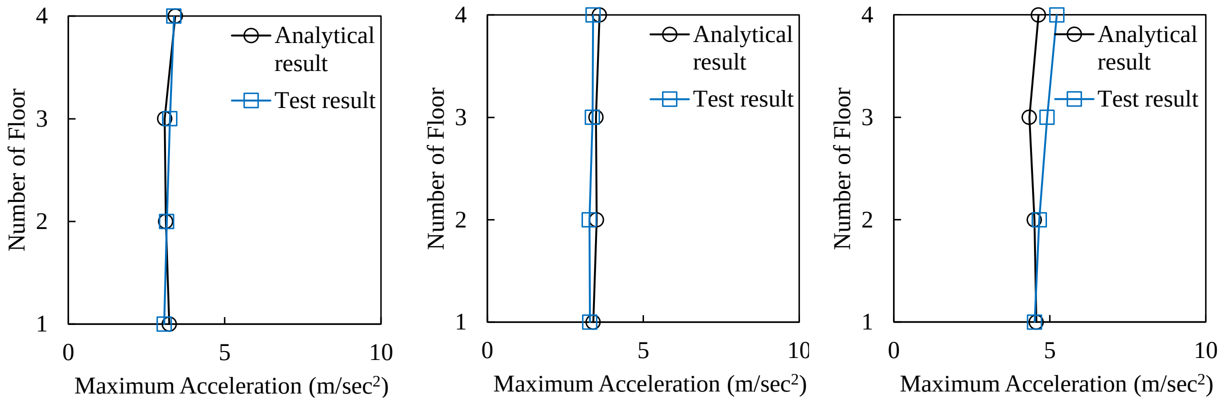

(a) Uni-direction

(b) Bi-direction (EW component)

(c) Bi-direction (NS component)

Figure 4.3. Response accelerations in case of SANNOMARU (200%)

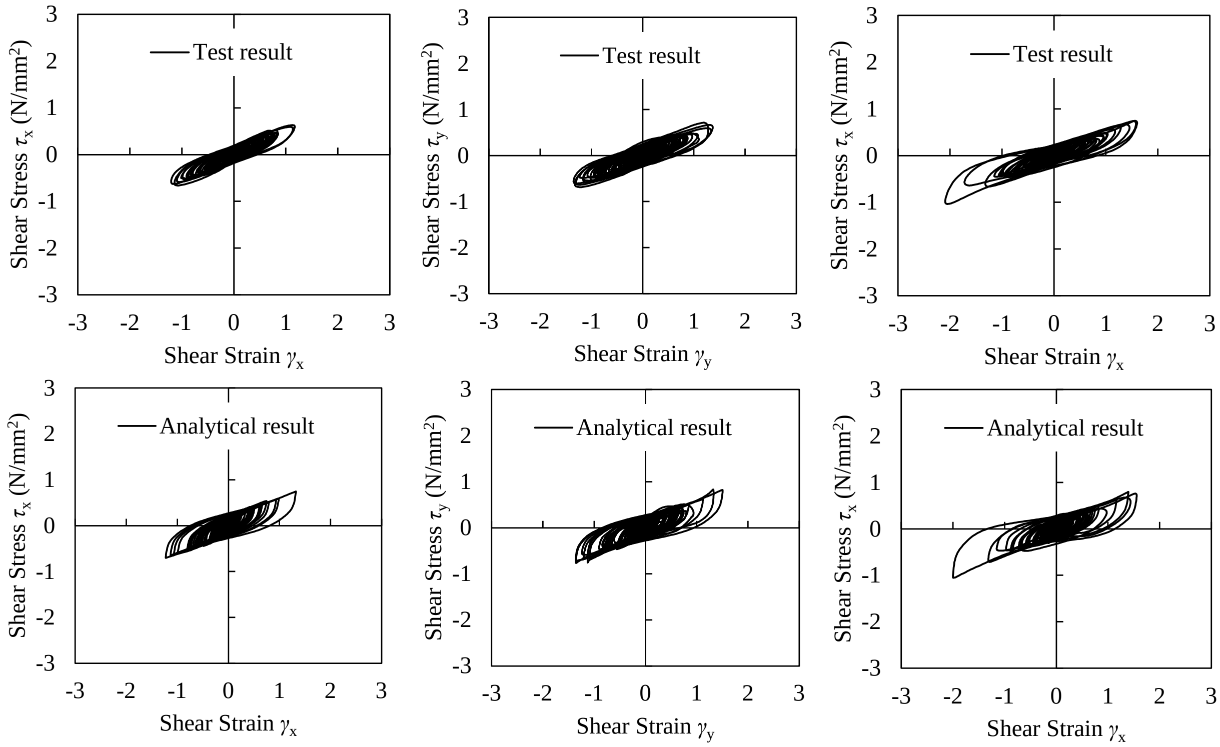

(a) Uni-direction

(b) Bi-direction (EW component)

(c) Bi-direction (NS component)

Figure 4.4. Stress-Strain relationships of HRB in case of SANNOMARU (200%).

5. CONCLUSIONS

In this study, the validity of the analytical model for time history response analysis corresponding to bi-directional loadings was examined through the experiment for HRBs under bi-directional loading. A new analytical model based on an elasto-plastic, integral type deformation-history constitutive law previously proposed by the authors was used. First the analytical model corresponding to bi-directional loading from the elasto-plastic constitutive law was derived. Next, bi-directional loading test and a shaking table test were conducted to obtain the data to show the validity of the proposed model, and then the material parameters for the analytical model were identified. Lastly, the reproducibility of the analytical model was evaluated by comparison of the results of the shaking table test of the seismically isolated structure and the analytical result with the proposed model. The following results are obtained:

- Test result verified the applicability of the developed analytical model with IDH constitutive law.
- Maximum response displacement under bi-directional excitation was larger than under uni-directional excitation in the case of SANNOMARU. The results indicate the importance of consideration for appropriate safety margin when only uni-directional analysis is carried out at design of seismically isolated structures.

AKNOWLEDGEMENT

This study is a part of joint research on base isolation system with high-damping rubber bearings by Bridgestone, National Taiwan University (NTU), and National Center for Research on Earthquake Engineering (NCREE). Earthquake simulator testing was conducted in NCREE, Taiwan. The authors would like to thank for the encouragement to all who related to this study. Bi-directional loading test in chapter 3 is a part of the activities of sub-committee for high-damping rubber bearings, the Japan Society of Seismic Isolation (JSSI). We greatly appreciate the useful suggestions given by the members of the committee.

REFERENCES

Wataru, Seki, Yoshihide, Fukahori, Yutaka, Iseda and Tsutomu, Matsunaga (1987). A Large-Deformation Finite-Element Analysis for Multilayer Elastomeric Bearings. *Rubber Chem. Technol.* **60: 5**, 856-869

Mineo, Takayama, Hideyuki, Tada and Ryuichi, Tanaka (1992). Finite-Element Analysis of Laminated Rubber Bearing Used in Base-Isolation System. *Rubber Chem. Technol.* **65: 1**, 46-63

Junji, Yoshida, Masato, Abe, Yozo, Fujino and Hiroshi, Watanabe (2004). Three-Dimensional Finite-Element Analysis of High Damping Rubber Bearings. *J. Eng. Mech.* **130: 5**, 607-621

Jennings, P. C. (1964). Periodic Response of a General Yielding Structure. *J.Eng. Mech. Div.* **90: 2**, 131-166

Masaru, Kikuchi and IAN, D. Aiken (1997). An analytical hysteresis model for elastomeric seismic isolation bearings. *Earthquake Engng. Struct. Dyn.* **26:2**, 215-231

Masashi, Yamamoto, Shigeo, Minewaki, Harumi, Yoneda and Masahiko, Higashino (2012). Nonlinear behavior of high-damping rubber bearings under horizontal bidirectional loading: full-scale tests and analytical modeling. *Earthquake Engng. Struct. Dyn.* (Published online)

Y. J. Park, Y. K. Wen and A. H-S. Ang (1986). Random vibration fo hysteretic systems under bi-directional ground motions. *Earthquake Engng. Struct. Dyn.* **14:4**, 543-557

Masato, Abe, Junji, Yoshida and Yozo, Fujino (2004). Multiaxial behaviors of laminated rubber bearings and their modeling. I: Experimantal study. *J. Struct. Eng.* **130:8**, 1119-1132

Masato, Abe, Junji, Yoshida and Yozo, Fujino (2004). Multiaxial behaviors of laminated rubber bearings and their modeling. II: Modeling. *J. Struct. Eng.* **130:8**, 1133-1145

Damian, N. Grant, Gregory, L. Fenves and Andrew, S. Whittaker (2004). Bidirectional modeling of high-damping rubber bearings. *J. Earthquake Eng.* **8:1**, 161-185

Takahiro, Mori, Hideaki, Kato, Takashi, Kikuchi and Nobuo, Murota (2011). *Elastic-plastic constitutive law of rubber for laminated rubber bearings. 12th World Conference on Seismic Isolation Energy Dissipation and Active Vibration Control of Structures.*

O. H. Yeoh (1993). Some forms of the strain energy function for rubber, *Rubber Chem. Technol.* **66: 5**, 754-771

R. W. Ogden (1998). Nonlinear Elastic Deformations, Dover

Hideaki, Kato, Yusuke, Samejima, Hiroyuki, Deura, Nobuo, Murota, Shigenobu, Suzuki, Kuo-Chun, Chang, Jenn-Shin, Hwang and Shiang-Jung, Wang (2009). Earthquake simulator testing of high-damping rubber bearings focused on bi-lateral force-displacement characteristics. *11th World Conference on Seismic Isolation Energy Dissipation and Active Vibration Control of Structures.*

Nakata, T., Fukuwa. N., Fujikawa, S., Dan, K., Sato, T., Shibata, Y., Shirase, Y. and Saito, K. (2004). Strong motion prediction for retrofit of buildings in the Sannomaru District of Nagoya City. *Summaries of Technical Papers of Annual Meeting AIJ B-2 structures II*, 529-534